

A two-Higgs-doublet interpretation of a small Tevatron Wjj excess

John F. Gunion

Department of Physics, University of California, Davis, CA 95616, USA

We show that a Wjj excess in Tevatron data could be explained in the context of the standard non-supersymmetric two-Higgs-doublet model (2HDM) for appropriately chosen parameters. Correlated signals in the $\gamma\gamma$ and $W^+W^-b\bar{b}$ final states are predicted and are on the verge of being detectable. The proposed model is most attractive if the cross section for the Wjj excess is $\lesssim 1 - 2$ pb.

PACS numbers:

The discrepancy between the CDF [1] and D0 [2] results implies considerable uncertainty as to whether there is an excess of Wjj events in the $M_{jj} \sim 140$ GeV region. Nonetheless, it is interesting to explore the different theoretical approaches that could produce such an excess. Many possibilities have appeared in the literature, including several Higgs sector approaches. A probably incomplete summary is the following: approaches based on $SU(2)$ doublet scalars with or without extra singlets [3–7]; Z -prime models [8, 9]; new colored state models [10–12]; supersymmetry models [13, 14]; technicolor models [15]; string theory models [16]; and within the context of the Standard model [17–19]. This Letter demonstrates that the excess could be explained by the simplest non-supersymmetric two-Higgs-doublet (2HDM) model *with completely standard Yukawa coupling structure*. The model predicts correlated signals in the $\gamma\gamma$ and $W^+W^-b\bar{b}$ final states that are on the verge of detection.

We begin with a general overview of the approach. We employ a two-Higgs-doublet model of Type-II (a convenient summary appears in the HHG [20]). In the context of the 2HDM, the masses of the light and heavy CP-even Higgs bosons, h and H , of the CP-odd Higgs boson, A , and of the charged Higgs boson H^\pm , as well as the value of $\tan\beta = v_u/v_d$ ($v_{u,d} = \langle H_{u,d}^0 \rangle$ where $H_{u,d}^0$ couple to up-type, down-type quarks, respectively) and the CP-even Higgs sector mixing angle α can all be taken as independent parameters, whose values will determine the λ_i of the general 2HDM Higgs potential.

To obtain a Wjj signal with Tevatron cross section of order $\gtrsim 1$ pb, the first ingredient is to note that the cross section for $gg \rightarrow A$ is highly enhanced at a given m_A relative to the cross section for a SM Higgs boson at $m_{h_{SM}} = m_A$ when $\tan\beta < 1$. The Wjj signal derives from the (dominant) $A \rightarrow H^\pm W^\mp$ decay channel with $H^\pm \rightarrow cs$. Note that this particular mode does not contain b quarks, as consistent with the CDF observations.¹ Using the predicted value of $BR(H^+ \rightarrow cs) \sim 0.2$ for $m_{H^\pm} \sim 140$ GeV when $\tan\beta$ is small, one finds that a cross section for $gg \rightarrow A \rightarrow H^\pm W^\mp \rightarrow csW^\mp$ as large

as the CDF value of ~ 4 pb can only be achieved for $m_A \in [250, 300]$ GeV if $\tan\beta \lesssim 1/10$, a domain for which the top-quark Yukawa coupling is non-perturbative, $\alpha_t \equiv \lambda_t^2/(4\pi) > 1$. However, a smaller Wjj cross section of order $1 - 2$ pb is possible for $\alpha_t \sim 1$. We now present more details.

In the 2HDM there are only two possible models for the fermion couplings that naturally avoid flavor changing neutral currents (FCNC), Model I and Model II. In Model II, our focus here, the tree-level couplings of the Higgs bosons are:

	h	H	A
$t\bar{t}$	$\frac{\cos\alpha}{\sin\beta}$	$\frac{\sin\alpha}{\sin\beta}$	$-i\gamma_5 \cot\beta$
$b\bar{b}$	$-\frac{\sin\alpha}{\cos\beta}$	$\frac{\cos\alpha}{\cos\beta}$	$-i\gamma_5 \tan\beta$
WW, ZZ	$\sin(\beta - \alpha)$	$\cos(\beta - \alpha)$	0

(1)

We will fix α relative to β by requiring that the h be SM-like, *i.e.* $\sin(\beta - \alpha) = 1$. We also choose $m_h = 115$ GeV for easy consistency with precision electroweak data. If the λ_i of the Higgs potential are kept highly perturbative, the decoupling limit, in which $m_H, m_{H^\pm} \rightarrow m_A$ and $\sin^2(\beta - \alpha) \rightarrow 1$, sets in fairly quickly as m_A increases [21]. To describe a Wjj excess requires that $m_{H^\pm} < m_A$ (but $m_H \sim m_A$ is useful to enhance the signal), implying that the decoupling limit does not apply at the masses of interest. This requires that several of the λ_i are substantial but still below the $\lambda_i^2/(4\pi) \sim 1$ beginning of the non-perturbative domain.

Looking at Eq. (1), it is apparent that the cross section for $gg \rightarrow A$ can be large when $\cot\beta > 1$. It is also useful to recall that the fermionic loop function for the A is substantially larger than that for the H (the CP-even Higgs that could contribute to the Wjj excess if the h is SM-like); *e.g.* asymptotically $F_{1/2}^A(\tau) \rightarrow 2$ in comparison to $F_{1/2}^H(\tau) \rightarrow -4/3$ when $\tau = 4m_f^2/m_A^2 \rightarrow \infty$, implying a cross section gain by a factor of $9/4$ for A vs. the H in the heavy fermion mass limit. We have computed the $gg \rightarrow A$ (and $gg \rightarrow H$) cross section using HIGLU [22] and a private program and obtained essentially the same results. Results for $\sigma(gg \rightarrow A)$ are plotted in Fig. 1. These results include NLO and NNLO corrections as in HIGLU. Some useful benchmark numbers for

¹ However, $H^\pm \rightarrow t^*b$ has a large branching fraction, as discussed later, but since $t^* \rightarrow Wb$, this channel will not lead to a jj resonance signal.

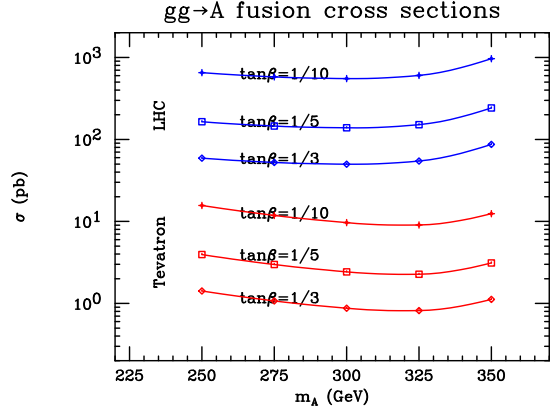


FIG. 1: Tevatron and LHC cross sections for $gg \rightarrow A$ for representative $\tan \beta < 1$ values.

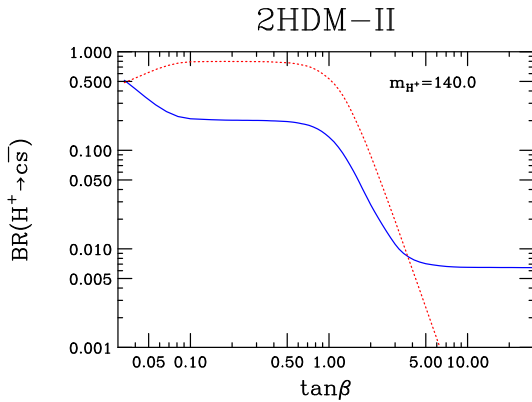


FIG. 2: $BR(H^+ \rightarrow c\bar{s})$ (solid blue) and $BR(H^+ \rightarrow t\bar{b})$ (red dots) as a function of $\tan \beta$ for $m_{H^\pm} = 140$ GeV and Model II couplings. Inclusion of off-shell decay configurations is essential for the $t\bar{b}$ final state.

$m_A = 250$ GeV are

$\tan \beta$	1/3	1/5	1/10
$\sigma(gg \rightarrow A)_{Tevatron}$	1.4 pb	3.9 pb	15.7 pb
$\sigma(gg \rightarrow A)_{LHC}$	59.1 pb	164.3 pb	652.9 pb

We define the effective Wjj cross section for a Higgs boson X :

$$\sigma_{Wjj}^X \equiv BR(X \rightarrow H^\pm W^\mp) BR(H^\pm \rightarrow c\bar{s}) \sigma(gg \rightarrow X), \quad (3)$$

where $X = A$ and $X = H$ are the relevant Higgs bosons. As a benchmark to keep in mind, we will suppose that $\sigma_{Wjj}^A \sim 1$ pb is appropriate for describing the Tevatron Wjj excess. $BR(H^+ \rightarrow c\bar{s})$ (computed privately and using HDECAY [23]) is displayed in Fig. 2 where we see that a value of ~ 0.22 applies for $\tan \beta \in [1/10, 1/3]$. For $m_A = 250$ GeV, Fig. 3 shows that $BR(A \rightarrow H^\pm W^\mp) \sim 0.95, 0.874, 0.64$ for $\tan \beta = 1/3, 1/5, 1/10$ (the solid green, magenta, blue

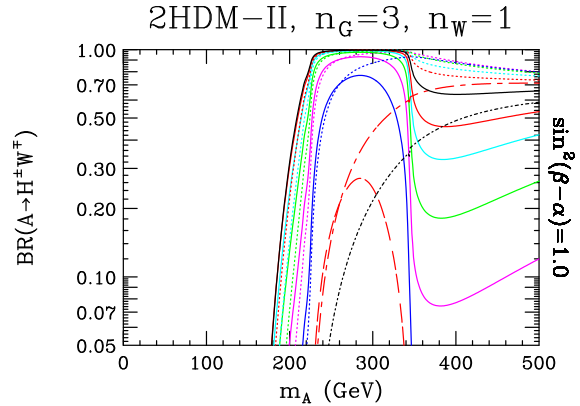


FIG. 3: $BR(A \rightarrow H^\pm W^\mp)$ as a function of m_A for $m_{H^\pm} = 140$ GeV and Model II couplings. In this and subsequent plot for the A , we have taken $m_H = 140$ GeV. The legend is as follows: solid black $\rightarrow \tan \beta = 1$; red dots $\rightarrow \tan \beta = 1.5$; solid red $\rightarrow \tan \beta = 1/1.5$; cyan dots $\rightarrow \tan \beta = 2$; solid cyan $\rightarrow \tan \beta = 1/2$; green dots $\rightarrow \tan \beta = 3$; solid green $\rightarrow \tan \beta = 1/3$; magenta dots $\rightarrow \tan \beta = 5$; solid magenta $\rightarrow \tan \beta = 1/5$; blue dots $\rightarrow \tan \beta = 10$; solid blue $\rightarrow \tan \beta = 1/10$; long red dashes plus dots $\rightarrow \tan \beta = 30$; pure long red dashes $\rightarrow \tan \beta = 1/30$; black dotdash $\rightarrow \tan \beta = 50$. This and subsequent figures must be viewed in color in order to resolve the different $\tan \beta$ cases. Results plotted include off-shell decay configurations. $n_G = 3, n_W = 1$ means 3 generations, no sequential W' .

lines), respectively. For $m_A = 250$ GeV we then obtain $BR(A \rightarrow H^\pm W^\mp) BR(H^+ \rightarrow c\bar{s}) \sim 0.21, 0.19, 0.14$ for $\tan \beta = 1/3, 1/5, 1/10$. Using the $\sigma(gg \rightarrow A)$ cross sections of Eq. (2), for $m_A = 250$ GeV we find $\sigma_{Wjj}^A(Tevatron) \sim 0.3$ pb, 0.75 pb, 2.2 pb for $\tan \beta = 1/3, 1/5, 1/10$, respectively. The corresponding values of α_t are 0.63, 1.75, 7. Only the latter is uncomfortably (but not drastically) non-perturbative, implying a preference for $\sigma_{Wjj}^A \lesssim 1$ pb. It is quite important to note that the main reason that σ_{Wjj}^A is not larger is the small value of $BR(H^+ \rightarrow c\bar{s})$ that is a consequence of the dominance of *off-shell* $H^+ \rightarrow t^* \bar{b}$ decays for $m_{H^\pm} = 140$ GeV. (This dominance decreases rapidly if m_{H^\pm} is decreased; for m_{H^\pm} significantly lower than 140 GeV higher σ_{Wjj}^A would thus be achieved.) For $m_A \gtrsim 300$ GeV, σ_{Wjj}^A is about 50% smaller than the $m_A = 250$ GeV values quoted above, see Fig. 1.

As apparent from Eq. (2), $\sigma(gg \rightarrow A)$ is much larger at the LHC. Focusing on $m_A = 250$ GeV and including the earlier quoted $BR(A \rightarrow H^\pm W^\mp) BR(H^+ \rightarrow c\bar{s})$ values of 0.21, 0.19, 0.14 we obtain $\sigma_{Wjj}^A(LHC) = 12.4$ pb, 31.2 pb, 91.4 pb for $\tan \beta = 1/3, 1/5, 1/10$, respectively. The number of Wjj events will be enormous for the soon-to-be-achieved $L = 1$ fb $^{-1}$. We anxiously await the appropriate LHC analyzes.

It is, of course, interesting to assess the extent to which $gg \rightarrow H \rightarrow H^\pm W^\mp$ with $H^+ \rightarrow c\bar{s}, H^- \rightarrow \bar{c}s$ could con-

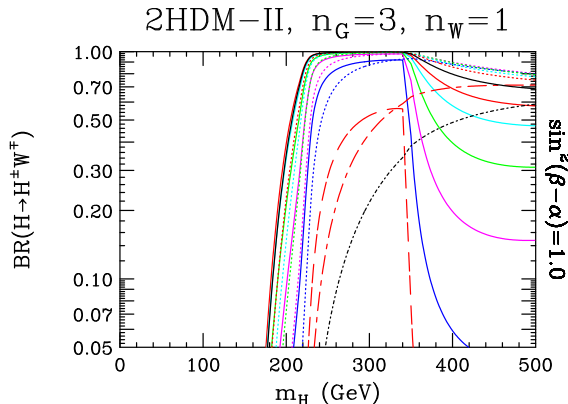


FIG. 4: $BR(H \rightarrow H^\pm W^\mp)$ as a function of m_A for $m_{H^\pm} = 140$ GeV and Model II couplings. In this and subsequent plots for the H , we have taken $m_A = 200$ GeV. The legend is as in Fig. 3.

tribute to the Wjj final state (recall that the h is taken to be light and SM-like so that only the H is relevant for the Wjj excess). We have already noted that $\sigma_{Wjj}^H < \sigma_{Wjj}^A$ due to the smaller fermionic loop function. Actual ratios at the Tevatron are: $\sigma_{Wjj}^A/\sigma_{Wjj}^H \sim 2.6, 3.0, 5.0$ for $m_A = m_H = 250, 300, 350$ GeV. Meanwhile, the $BR(H \rightarrow H^\pm W^\mp)BR(H^+ \rightarrow c\bar{s})$ values are similar to those quoted for the A . Thus, for the preferred $m_H \in [250 - 300]$ GeV mass range, the H would yield a Wjj signal of order 30% – 40% of the A result. If the H and A are not fairly degenerate, this would yield a somewhat spread out net Wjj signal, despite the $\lesssim 1$ GeV total widths of the A and H (for the $\tan\beta$ values being discussed), given the experimental M_{jj} resolution of order 15 GeV. This is perhaps suggested by the absence of any distinct peaking in the Wjj mass in the data. Another interesting point is that in this model with m_H not very different from m_A , there would be no signal in the Zjj channel due to the absence of $H \rightarrow AZ$ and $A \rightarrow HZ$ decays.

Other signals should be seen if the model is correct. In particular, as pointed out in [24], there is a very large $A \rightarrow \gamma\gamma$ signal for small $\tan\beta$. A plot of $R_{\gamma\gamma}^A \equiv [\Gamma_{gg}^A BR(A \rightarrow \gamma\gamma)]/[\Gamma_{gg}^{h_{SM}} BR(h_{SM} \rightarrow \gamma\gamma)]$ is given in Fig. 5. For $\tan\beta \sim 1/3, 1/5$ and $m_A \sim 250$ GeV, $R_{\gamma\gamma}^A \sim 10^2, 10^3$, respectively! Such a signal will soon be observed at the LHC if present and might also be observable with current Tevatron data. To assess actual event rates one can combine the actual branching ratio for $A \rightarrow \gamma\gamma$, plotted in Fig. 6 with the cross sections for $gg \rightarrow A$ plotted in Fig. 1.

For example, for $\tan\beta = 1/5$ and $m_A = 250$ GeV, in the case of the Tevatron one finds $\sigma(gg \rightarrow A)BR(A \rightarrow \gamma\gamma) \sim 3.9 \text{ pb} \times 4.8 \cdot 10^{-4} \simeq 1.9 \times 10^{-3} \text{ pb}$, yielding ~ 10 events for $L = 5.4 \text{ fb}^{-1}$. This must be compared to the number of events expected in the SM. Ref. [25] performs an analysis for $L = 5.4 \text{ fb}^{-1}$. Their net efficiency

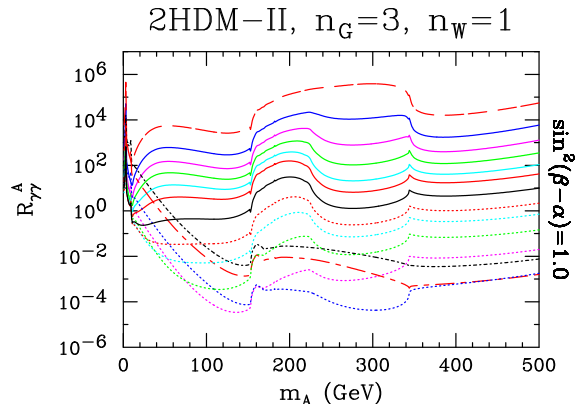


FIG. 5: $R_{\gamma\gamma}$ for the 2HDM-II A . The legend is as in Fig. 3. This figure takes account of all the A decay modes, including especially $A \rightarrow H^\pm W^\mp$ as well as $A \rightarrow t\bar{t}$ (off-shell) decays.

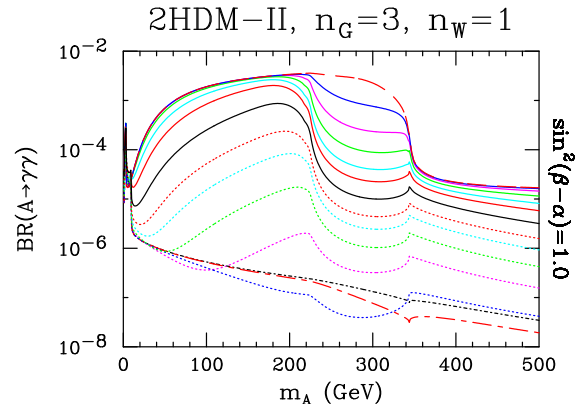


FIG. 6: $BR(A \rightarrow \gamma\gamma)$ for the 2HDM-II A after including $A \rightarrow H^\pm W^\mp$ and $A \rightarrow t\bar{t}$ off-shell decays in the present scenario. The legend is as in Fig. 3.

times acceptance is ~ 0.12 , implying a predicted number of $A \rightarrow \gamma\gamma$ events of order 1.2. The actual number of observed events is consistent with the SM prediction, as shown in their Fig. 2. They set a 95% CL limit of $\sigma BR(\gamma\gamma) \lesssim 0.05 \text{ pb}$ at $M_{\gamma\gamma} = 250$ GeV, a factor of ~ 25 above our typical prediction. At the LHC, the corresponding calculation is $\sigma(gg \rightarrow A)BR(A \rightarrow \gamma\gamma) \sim 164 \text{ pb} \times 4.8 \cdot 10^{-4} = 0.08 \text{ pb}$. For $L = 36 \text{ pb}^{-1}, 1 \text{ fb}^{-1}$ this yields $\sim 3, 80$ events, respectively. Ref. [26] uses $L = 36 \text{ pb}^{-1}$ data to set a limit of $\sigma \times BR(\gamma\gamma) \lesssim 0.7 \text{ pb}$ at $M_{\gamma\gamma} = 250$ GeV, a factor of about 8 above the prediction for the present scenario. This shows that the present scenario for obtaining a Wjj excess will be strongly tested once the currently available LHC data sets with $L = 1 \text{ fb}^{-1}$ are analyzed.

Of course, the H also yields a large $\gamma\gamma$ signal (again of order 30% – 40% that of the A) that most probably would be detected as a separate peak if m_H differs from

m_A by more than 10 GeV, given the excellent ~ 2 GeV mass resolution in $M_{\gamma\gamma}$ for the LHC detectors and given that the total A and H widths are of order 1 GeV.

Finally, there is an interesting signal in the $gg \rightarrow A \rightarrow H^\pm W^\mp \rightarrow t^* \bar{b} W^- + \bar{t}^* b W^+$ final state deriving from the $BR(H^+ \rightarrow t^* \bar{b}) \sim 0.7$ (off-shell) decays, see Fig. 2, where $t^* \rightarrow W^+ b$. The resulting final states of $W^+ W^- b \bar{b}$ will not peak in either Wb mass combination. The cross section for this final state is, however, significant: for $m_A = 250$ GeV and $\tan\beta = 1/5$, one finds $\sigma(WWb\bar{b}) \sim 2.8$ pb compared to $\sigma_{Wjj}^A \sim 0.75$ pb and $\sigma_{Wjj}^H \sim 0.28$ pb. Although this $\sigma(WWb\bar{b})$ is somewhat smaller than that for direct $t\bar{t} \rightarrow W^+ W^- b \bar{b}$ production, it is still sizable and might lead to some ‘‘anomalies’’ in the $W^+ W^- b \bar{b}$ final state. It would be very interesting to determine whether or not such anomalies in the $W^+ W^- b \bar{b}$ final state would have been noticed in current data and, if not, how much LHC integrated luminosity would be needed to detect them. One should note that for this model to achieve the CDF Wjj cross section of ~ 4 pb would imply an anomalous $W^+ W^- b \bar{b}$ final state cross section that is larger than that coming directly from $t\bar{t} \rightarrow W^+ W^- b \bar{b}$ production.

If a 4th generation is present with $m_{t',b'} \sim 400$ GeV, then Γ_{gg}^A and, therefore, σ_{Wjj}^A is increased substantially at any fixed $\tan\beta$. However, $\tan\beta$ is restricted to lie in the range $\tan\beta \in [1/2, 2]$ in order to keep $\lambda_{t',b'}^2/(4\pi) \lesssim 1$. The resulting $gg \rightarrow A$ rate is then more or less the same as for $\tan\beta \in [1/3, 1/5]$ with no 4th generation.

Enhanced $gg \rightarrow A$ cross sections also arise in a Model I 2HDM if $\tan\beta < 1$. However, the enhancement is not quite as great as for Model II. In addition, $BR(H^+ \rightarrow c\bar{s}) \sim 0.13$ for $\tan\beta \in [1/3, 1/10]$. As a result, the Wjj cross section that can be achieved in Model I is smaller by about a factor of three as compared to that achieved

for the Wjj final state in the case of Model II.

To summarize, we have shown that if $\tan\beta$ is small then a Model II two-Higgs-doublet sector with m_A , and possibly m_H , of order 250 GeV – 300 GeV can lead to a very interesting signal in the Wjj final state that could match that seen by CDF at the Tevatron. To get a cross section as large as that originally claimed by CDF would force one to $\tan\beta \lesssim 1/10$, values for which the top-quark Yukawa coupling is quite large and moderately non-perturbative. However, a Wjj signal with cross section of order 1 pb, as possibly consistent with a combination of CDF and D0 data, is quite possible without entering into the domain of non-perturbative top-quark Yukawas. Correlated signals in the $W^+ W^- b \bar{b}$ and $\gamma\gamma$ final states are expected. These final states are interesting targets for exploration in their own right. The predicted correlations between the Wjj , $W^+ W^- b \bar{b}$ and $\gamma\gamma$ signals makes the model proposed herein highly testable and points out the importance of taking into account the latter types of signals in order to fully assess the consistency of the model. At the LHC, the predicted Wjj cross sections and those for the correlated signals are of order 40 times as large as at the Tevatron. As the integrated LHC luminosity approaches $L = 1 \text{ fb}^{-1}$ the model will most probably be definitively eliminated or confirmed. As a final note, the masses for the m_{H^\pm} , m_A and m_H needed to explain the possible Wjj excess using the approach described here cannot be achieved within the minimal supersymmetric model context.

Acknowledgments

JFG is supported by U.S. DOE grant No. DE-FG03-91ER40674. Thanks to S. Chang for a critical examination of the paper and helpful comments.

-
- [1] T. Aaltonen *et al.* [CDF Collaboration], Phys. Rev. Lett. **106**, 171801 (2011), arXiv:1104.0699.
 - [2] V. M. Abazov *et al.* [D0 Collaboration], arXiv:1106.1457.
 - [3] Q. H. Cao, M. Carena, S. Gori, A. Menon, P. Schwaller, C. E. M. Wagner and L. T. M. Wang, arXiv:1104.4776.
 - [4] K. S. Babu, M. Frank, S. K. Rai, arXiv:1104.4782.
 - [5] B. Dutta, S. Khalil, Y. Mimura, Q. Shafi, arXiv:1104.5209.
 - [6] G. Segre, B. Kayser, arXiv:1105.1808.
 - [7] C. H. Chen, C. W. Chiang, T. Nomura and Y. Fusheng, arXiv:1105.2870.
 - [8] M. R. Buckley, D. Hooper, J. Kopp and E. Neil, arXiv:1103.6035.
 - [9] K. Cheung and J. Song, arXiv:1104.1375.
 - [10] X. P. Wang, Y. K. Wang, B. Xiao, J. Xu and S. h. Zhu, arXiv:1104.1917.
 - [11] B. A. Dobrescu and G. Z. Krnjaic, arXiv:1104.2893.
 - [12] L. M. Carpenter, S. Mantry, arXiv:1104.5528.
 - [13] C. Kilic and S. Thomas, arXiv:1104.1002.
 - [14] R. Sato, S. Shirai and K. Yonekura, arXiv:1104.2014.
 - [15] E. J. Eichten, K. Lane and A. Martin, arXiv:1104.0976.
 - [16] L. A. Anchordoqui, H. Goldberg, X. Huang, D. Lust and T. R. Taylor, arXiv:1104.2302.
 - [17] X. G. He and B. Q. Ma, arXiv:1104.1894.
 - [18] Z. Sullivan, A. Menon, arXiv:1104.3790.
 - [19] T. Plehn, M. Takeuchi, arXiv:1104.4087.
 - [20] *The Higgs Hunters Guide*, John F. Gunion, Howard E. Haber, Gordon Kane, Sally Dawson. 1990. Series: Frontiers in Physics, 80; QCD161:G78
 - [21] J. F. Gunion, H. E. Haber, Phys. Rev. **D67**, 075019 (2003), [hep-ph/0207010].
 - [22] M. Spira, Nucl. Instrum. Meth. A **389**, 357 (1997) [arXiv:hep-ph/9610350], arXiv:hep-ph/9510347.
 - [23] A. Djouadi, J. Kalinowski, M. Spira, Comput. Phys. Commun. **108**, 56-74 (1998), [hep-ph/9704448].
 - [24] J. F. Gunion, arXiv:1105.3965.
 - [25] T. Aaltonen *et al.* [CDF Collaboration], Phys. Rev. **D83**, 011102 (2011). [arXiv:1012.2795].
 - [26] CMS Collaboration, CMS PAS EXO-10-019.